

# **Performance Analysis of an Inertial Navigation Algorithm with DVL Auto-Calibration for Underwater Vehicle**

**A. Rossi, M. Pasquali, M. Pastore**

GEM Elettronica, Photonic Research & Advanced Navigation Science

Via A. Vespucci 9

63074 San Benedetto del Tronto (AP),

ITALY

Inertial Sensors and Systems 2014

Karlsruhe, Germany

## **Abstract**

Autonomy and high accuracy are fundamental for underwater navigation. For this reason, new inertial algorithms are under intensive investigation to improve the performances. In this paper, we present the INS/DVL calibration algorithm developed by GEM Elettronica for underwater applications. With this procedure, we improve the sensor data fusion between our unit, Doppler Velocity Log (DVL) and the GNSS receiver, moving along a well-defined trajectory. Acquired experimental data validate our simulation model, confirming our previously supposed results.

## **1. Introduction**

Inertial Navigation System (INS) is an inertial system that estimates the vehicle's position, attitude, and velocity as a function of time in the specified navigation frame. These informations are estimated using the outputs of an Inertial Measurement Unit (IMU), a reference clock and a model of the gravitational field [1]. An IMU is a device able to accurately measure rotation rates and accelerations of the platform on which it is installed. An IMU usually consists of three gyroscopes and three accelerometers to take in account of the six degrees of freedom of a platform in space.

A Strapdown Inertial Navigation System (SINS) based on Kalman filter (see Section 3.2) is a dead reckoning method widely used to provide attitude, velocity and position for underwater vehicle. Without external sensors aiding, an inertial navigation system based only on IMU have a position error drift growing over time. Significant advances have recently improved new INS algorithms and sensor integration for underwater navigation.

A mature technique to obtain position and velocity information is the combination of inertial navigation data and Global Navigation Satellite Systems (GNSS) data, which provides real time position information, time independent error and accuracy sufficient for navigation. The GNSS positioning update is possible only when the underwater vehicle is not submerged or electromagnetic interferences are not present. Therefore, other self-contained sensing techniques are required.

Doppler Velocity Log (DVL) can offer the speed relative to the seabed in DVL body frame. The INS uses this information as a valid aid to reduce the position and velocity errors due to integration over time.

In this paper a new INS algorithm, developed by GEM Elettronica for underwater applications, is used in a GPS/INS/DVL navigation system. Strapdown INS, DVL and GPS receiver are mounted on an underwater vehicle and are located with different lever arms. The accuracy problem relative to sensors misalignment is here investigated, since in the INS/DVL integrated navigation system misalignment angles, and DVL scale factor, are the principal position error source in inertial navigation. The calibration procedure between INS and DVL is a fundamental step in error reduction, since the mechanical misalignment estimation allows correction and compensation of DVL errors. In particular, moving the vehicle along a well-defined trajectory, the motion information acquired with inertial sensors aided by external GPS signals can be compared with the measured DVL information, allowing to estimate the misalignments.

During the movements that characterize the calibration process, external information measured by GPS must be present. Therefore, in this phase, the antenna of GPS receiver must be in a receiving position.

We use the term “auto-calibration” because this estimation of the parameters can be performed in real-time and inside the INS (without the aiding of external software or hardware), only needing an operator that executes the defined trajectory.

This paper is organized in two parts: in the first part we report the simulation data, pointing out the different aspects of our calibration algorithm.

In the second part we also show the experimental data obtained in a manned underwater vehicle. GEM Elettronica mounted its Inertial Navigation System (FOG-100 INS/S) in a 10 meters submersible vehicle. We analyse our system performance during experimental tests conducted in open sea. Acquired experimental data validate our simulation model, confirming our previously supposed results.

## **2. Fiber Optic Gyroscopes solutions**

The GEM Elettronica manufactured Fiber Optic Gyroscopes (FOG) are used in Navigation, Mining and Land application. GEM Elettronica has been developing his IMU and Attitude/Heading Reference System (AHRS) products for almost 10 years. Since 2008 it has been present on the FOG market and in 2013 new Photonic Research & Advanced

Navigation Science (PRANS) Laboratories were launched in the Italian company headquarters.

Polaris FOG-100, with the proprietary INS algorithm for underwater applications, achieves the specifications required for this mission.

Bias Instability	$5 \cdot 10^{-3} \text{ }^\circ/\text{h}$
Angle Random Walk	$3 \cdot 10^{-3} \text{ }^\circ/\sqrt{\text{h}}$
Rate Random Walk	$1 \cdot 10^{-2} \text{ }^\circ/\text{h}/\sqrt{\text{h}}$

Table 1: Noises magnitude of a typical FOG-100 fiber optic gyroscope.

The GEM Elettronica Polaris family is also composed of FOG-50 and FOG-200. We present their specifications in the following table.


	FOG-50	FOG-100/INS/M/S	FOG-200/INS/M/S
			
Heading	0.4° Sec(Lat) RMS	0.2° Sec(Lat) RMS	0.1° Sec(Lat) RMS
Roll/Pitch	0.1° RMS	0.05° RMS	0.018° RMS
Position (pure inertial)	-	3.5NM/12h CEP	2NM/12h CEP
Position (with LOG aiding)	-	1.8NM/12h CEP	1NM/12h CEP
Heave	5cm or 5% whichever is greater		
Settling time	≤ 10min (static) ≤ 30min (full accuracy, all conditions)		
Inputs	GPS, Pulse Log, NMEA Log, DVL		

Table 2: Polaris FOG family specifications.

### 3. Calibration Method

#### 3.1. DVL calibration parameters

The calibration parameters estimated in the calibration procedure are:

- the DVL misalignment angles  $(\alpha, \beta, \gamma)$  with respect to the INS frame
- the DVL scale factor  $(k)$

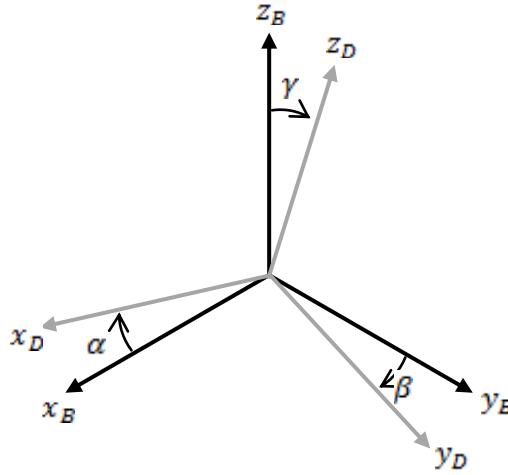
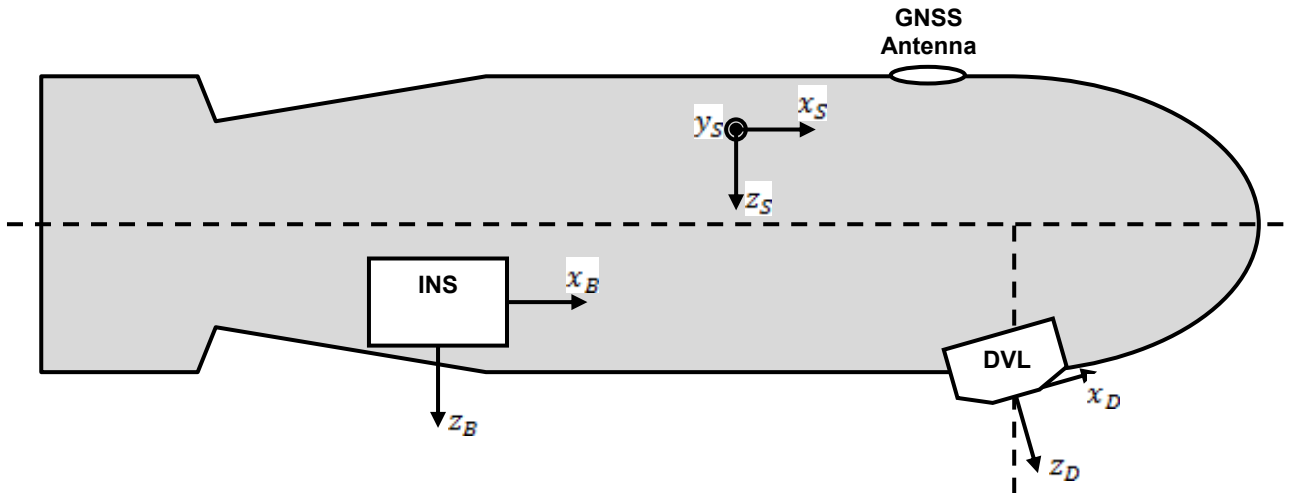


Figure 1: Misalignment angles between INS/Body and DVL reference systems.

We suppose that the INS/Body frame  $B$  is aligned with the vehicle frame  $S$ , and that all sensors are rigidly mounted. The DVL frame  $D$  is rotated with respect to body axis by some unknown angles. In the following figure, subscripts indicate the frame of reference.

Figure 2: A submarine sensors configuration. All sensors are rigidly attached to the



vehicle.

The following figures were generated running our algorithm following a test trajectory in a simulated environment (explained in Section 3.5), *without* GPS aiding. The only differences are the INS/DVL misalignment angles of  $(-1.6^\circ, 1.5^\circ, 2.3^\circ)$ .

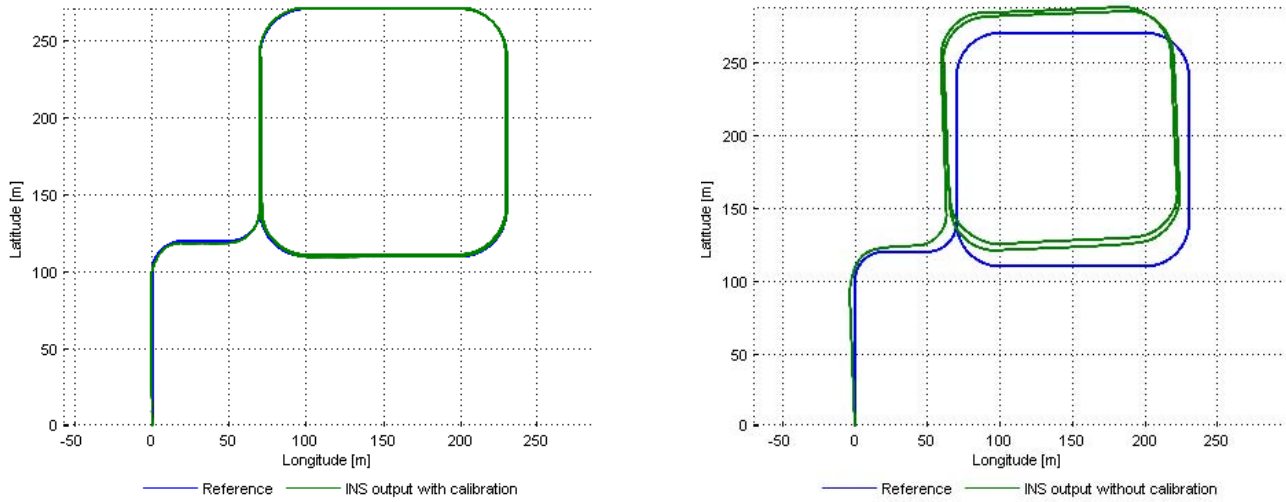


Figure 3: Comparison of position estimation with and without INS/DVL calibration.

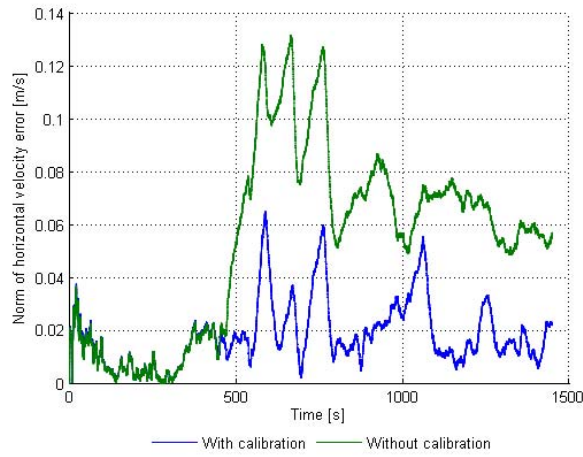


Figure 4: Velocity estimation error with and without INS/DVL calibration. Note that the norm of the real velocity is 1.5 m/s.

From Figure 3 and Figure 4 it is clear that without a proper calibration, the performance of the navigation system drop significantly.

In the next section we present our calibration method. As we will see, it consists in an online parameter estimation with a *Kalman Filter* running inside the FOG-100/INS, performed following a *well-defined trajectory*.

### 3.2. Internal algorithm structure

Kalman filter is a recursive state estimation algorithm, widely used in inertial navigation, guidance and control of vehicles, that produces the optimal estimate of a linear system state with gaussian and independent noisy input data.

Roughly speaking, the algorithm is composed of two main steps: *Time Propagation* and *Observational Update*. In the first step the current state variables are estimated, along with their uncertainties, using only their previously calculated value. Then, in the second step, whenever a measurement (noisy or corrupted by some error source) is observed, the filter updates these estimates using a sort of recursive weighted average, with more weight being given to estimates with higher certainty. We refer to [2], [3] and [4] for a more precise description of the filter and further details.

In the following diagram we illustrate the basic structure of our setup.

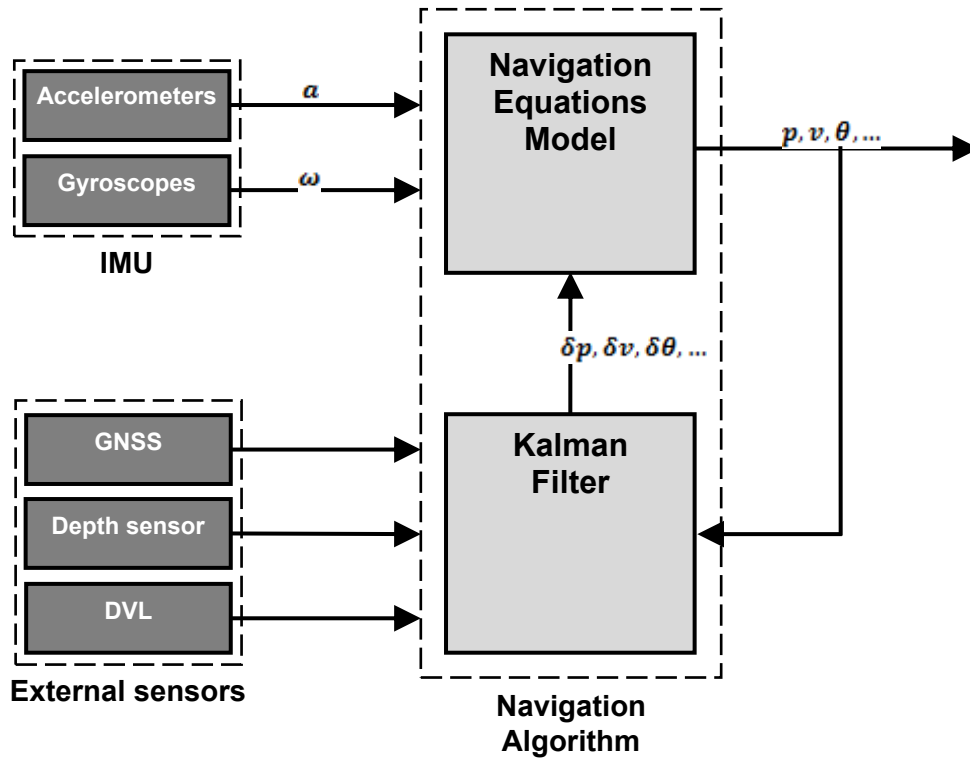


Figure 5: A closed-loop loosely coupled INS/GNSS/DVL integration scheme.

The Inertial Measurement Unit (IMU) sends accelerations  $\mathbf{a}$  and rotation rates  $\boldsymbol{\omega}$ , measured by accelerometers and gyroscopes, to the Navigation Equations Model. This block calculates position, velocity, attitude  $(\mathbf{p}, \mathbf{v}, \boldsymbol{\theta})$ , along with other internal states, such as sensors biases and scale factors. Afterwards, the Kalman Filter block calculates the state corrections  $(\delta \mathbf{p}, \delta \mathbf{v}, \delta \boldsymbol{\theta}, \dots)$  using the noisy input data provided by external sensors, such as GNSS position (in a loosely coupled approach), depth, and DVL velocity. These corrections will be then used to achieve a better estimation of the output variables.

### 3.3. Kalman Filter Observational Update

In this section we present the equation that constitute the calibration part of the Observational Update of Kalman Filter.

First we fix some notations: we indicate with  $\mathbf{x}$  the true value of a vector, with  $\hat{\mathbf{x}}$  the estimated value. We denote with  $\mathbf{N}$  the North-East-Down frame. The rotation matrix from a frame  $\mathbf{X}$  to a frame  $\mathbf{Y}$  will be denoted with  $\mathbf{C}_X^Y$ . Moreover, the INS attitude will be indicated with  $\theta_N$ , while  $\varphi_B$  will be the vector representing the rotational angles between the DVL and INS/Body frame.

The equation that links the INS *true* velocity  $\mathbf{v}_{INS}^N$  in the NED frame and the DVL *measured* velocity  $\mathbf{v}_{DVL}^D$  in its own frame is:

$$(1 + k)\mathbf{v}_{DVL}^D = \mathbf{C}_B^D \mathbf{C}_N^B \mathbf{v}_{INS}^N \quad (1)$$

where  $k$  is the *true* DVL scale factor. We suppose that the rotation matrix  $\mathbf{C}_D^B$  and the scalar  $k$  are both constants.

After some algebraic manipulation we obtain the Kalman filter Observational Update equation in its standard form [2, p. 138]

$$\mathbf{z} = \mathbf{H}\mathbf{x} \quad (2)$$

where

- $\mathbf{z}$  is 3-dimensional vector, function of the measured DVL velocity  $\mathbf{v}_{DVL}^D$ ;
- $\mathbf{H}$  is a 3 by 13 matrix, function of  $\hat{\mathbf{C}}_B^D, \hat{\mathbf{C}}_N^B, \hat{\mathbf{v}}_{INS}^N$  and  $\mathbf{v}_{DVL}^D$ ;
- $\mathbf{x}$  is the state 13-dim vector, i.e.  $\mathbf{x} = (\hat{p}, \hat{\mathbf{v}}_{INS}^N, \hat{\theta}_N, \hat{\varphi}_B, \hat{k})$ .

### 3.4. Calibration trajectories

We analyse different calibration trajectories, with the same length, travelled at the same velocity, and with the following shape:

- TRAJ01: snake shaped
- TRAJ02: square/rectangle shaped
- TRAJ03: eight shaped



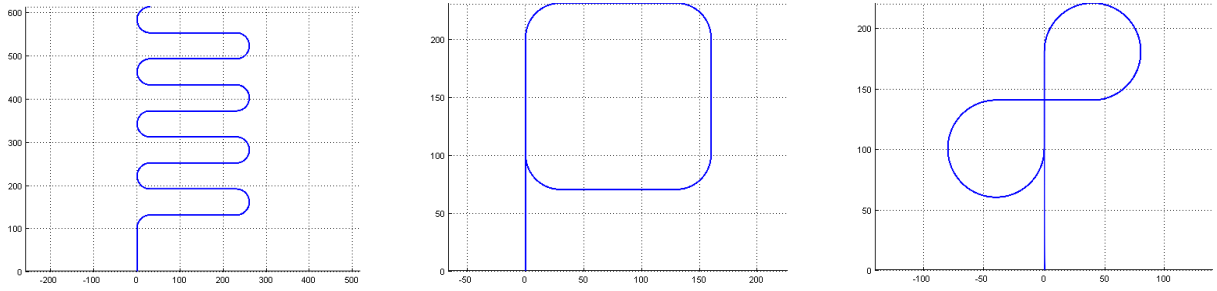


Figure 6: Examples of trajectories. From left to right: TRAJ01, TRAJ02, TRAJ03.

In every trajectory there is no immersion or emersion, since we are interested in surface paths where the INS can receive GNSS input data. Moreover, we do not need a measurement of depth in our calibration, even if it is usually available via a water pressure sensor.

Note that we do not consider a “straight” trajectory as a valid alternative. In fact, for the instantaneous observability (see [5] and [6]), curves and non-constant axial accelerations are fundamental to achieve the best possible estimate of misalignment angles.

### 3.5. Simulation framework

To make the test more robust we made a configurable test framework, in which we generate the trajectory by the concatenation of curves, accelerations, straight lines, etc. Every trajectory portion parameters can be perturbed by a random variable, so we can further expand our test set.

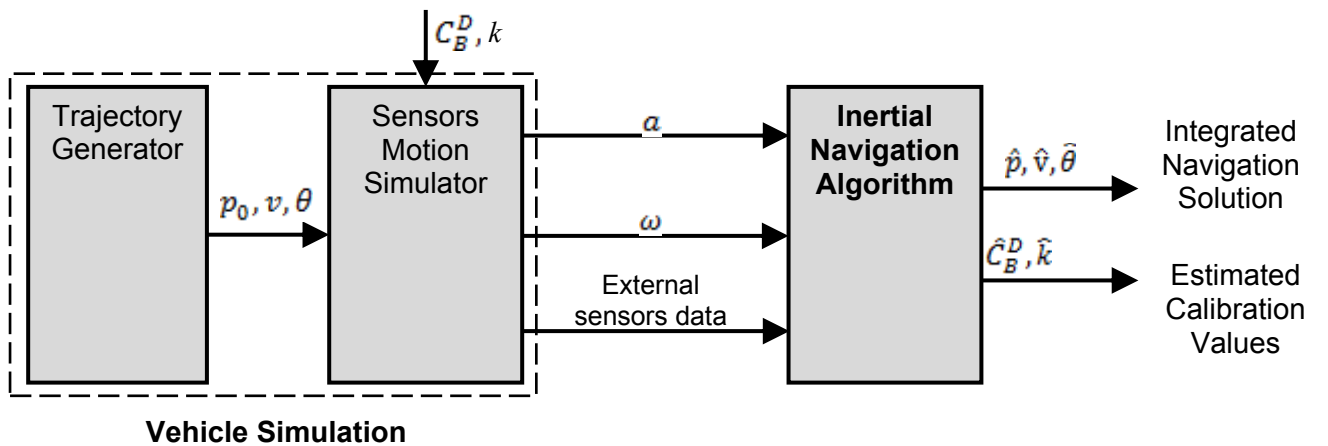


Figure 7: Simulation framework scheme.

In every simulation test, we generate the trajectory by calculating ideal attitude  $\theta$  and velocity  $v$  starting from a known position  $p_0$ . The trajectories generated are always smooth

(continuously infinitely differentiable). Then we calculate the sensors measurements with their relative errors and noises (accelerations  $\mathbf{a}$ , angular velocity  $\boldsymbol{\omega}$ , external sensors data such as GPS, DVL, depth, ...). With the inertial navigation algorithm we obtain an integrated navigation solution that incorporates position, velocity, and attitude ( $\hat{\mathbf{p}}$ ,  $\hat{\mathbf{v}}$ ,  $\hat{\boldsymbol{\theta}}$ ), and the estimated DVL calibration parameters  $\hat{\mathbf{C}}_B^D, \hat{\mathbf{k}}$ .

We simulate the effect of the waves in a medium-calm sea condition. We do not simulate the effect of sea currents and wind because we suppose to have maximum satellite visibility with our GNSS receiver, so that we can correct the INS position with an absolute measurement. In addition, we suppose to be always in sea bottom tracking, so that the DVL has always a ground-referenced velocity output.

Finally, we remark that this calibration method is independent from GPS signal quality, and nothing happens if GPS position fix is lost for a short time.

### 3.6. Simulation results

In the first test set, we analyse each trajectory type with the Monte Carlo method, following these rules:

- every sensor noises (GPS, DVL, IMU accelerometers and gyroscopes) may vary within each nominal specification;
- DVL mounting angles may vary uniformly between  $\pm 5^\circ$ , while the DVL scale factor normally with a standard deviation of 7%;
- the ideal speed and total distance travelled are fixed, respectively at 3 knots (about 1.5 m/s) and about 2400 m.

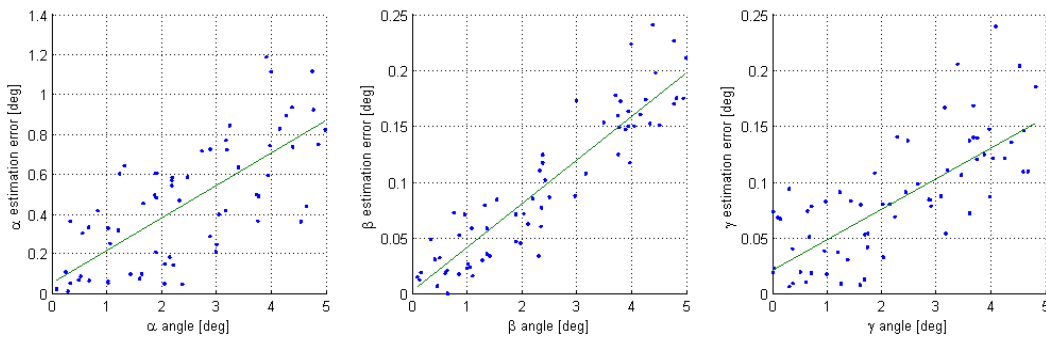


Figure 8: TRAJ01 misalignment angles estimation error.

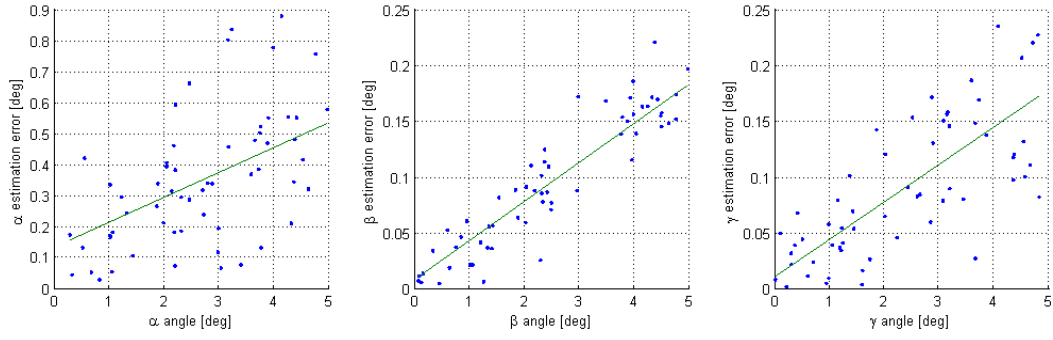


Figure 9: TRAJ02 misalignment angles estimation error.

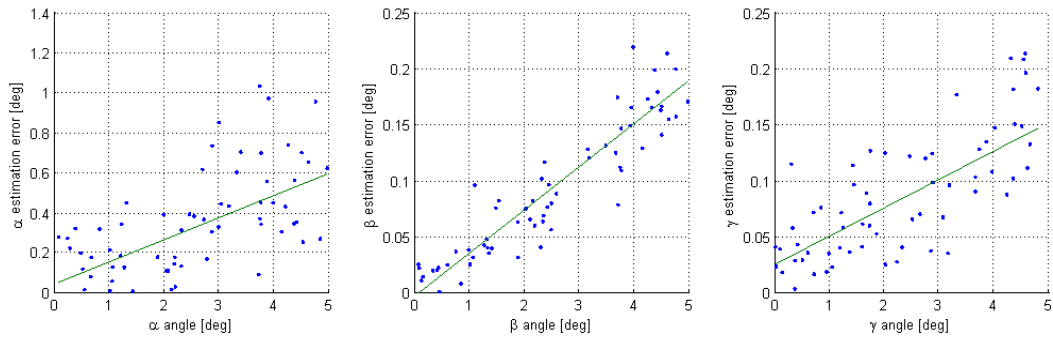


Figure 10: TRAJ03 misalignment angles estimation error.

From this first analysis we obtain that the trajectory achieving the best estimation of the misalignment angles is TRAJ03, as we can see in the following table.

Trajectory	Mean [deg]	Standard Deviation [deg]
TRAJ01	0.50	0.28
TRAJ02	0.39	0.18
TRAJ03	0.36	0.22

Table 3: Norm of misalignment angles estimation error: mean and standard deviation (1<sup>st</sup> test set).

The same holds for the scale factor estimation.

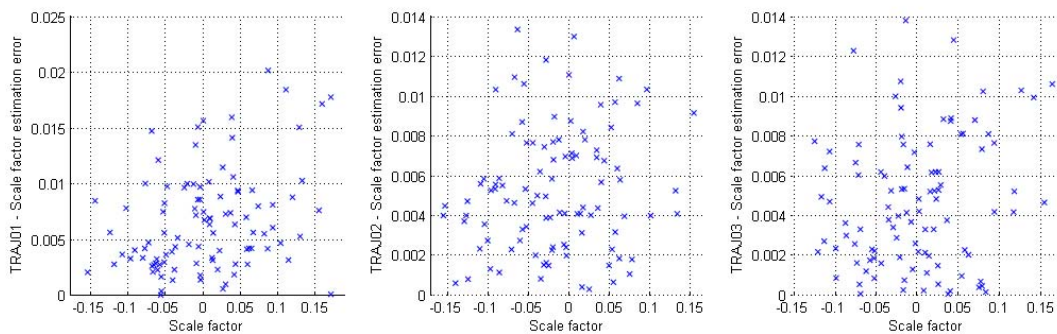


Figure 11: Scale factor estimation error.

Trajectory	Mean	Standard Deviation
TRAJ01	0.0066	0.0044
TRAJ02	0.0052	0.0031
TRAJ03	0.0046	0.0032

Table 4: Scale factor estimation error: mean and standard deviation (1<sup>st</sup> test set).

Next, in the second test set we fix the DVL misalignment angles and we geometrically alter each part of the trajectory, in order to evaluate the robustness of our algorithm in each case.

In particular

- every sensor noise (GPS, DVL, IMU accelerometers and gyroscopes) may vary within each nominal specification;
- the DVL mounting angles are  $(2.5^\circ, 2.5^\circ, 2.5^\circ)$  and the DVL scale factor is 7%;
- the ideal speed may vary between 1.3 m/s and 2 m/s.

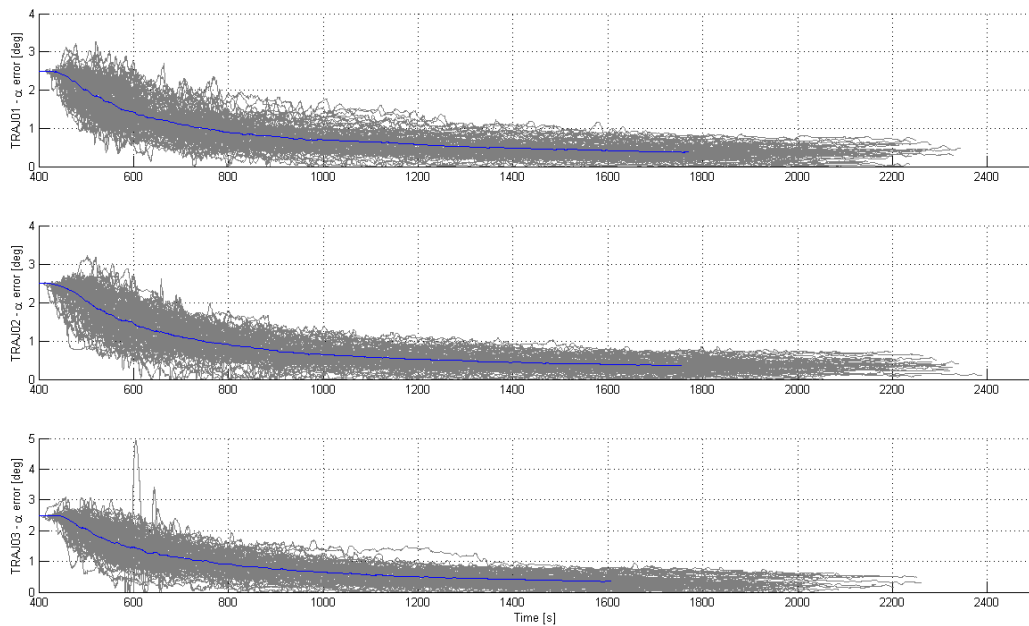


Figure 12:  $\alpha$  misalignment angle estimation error in each test.

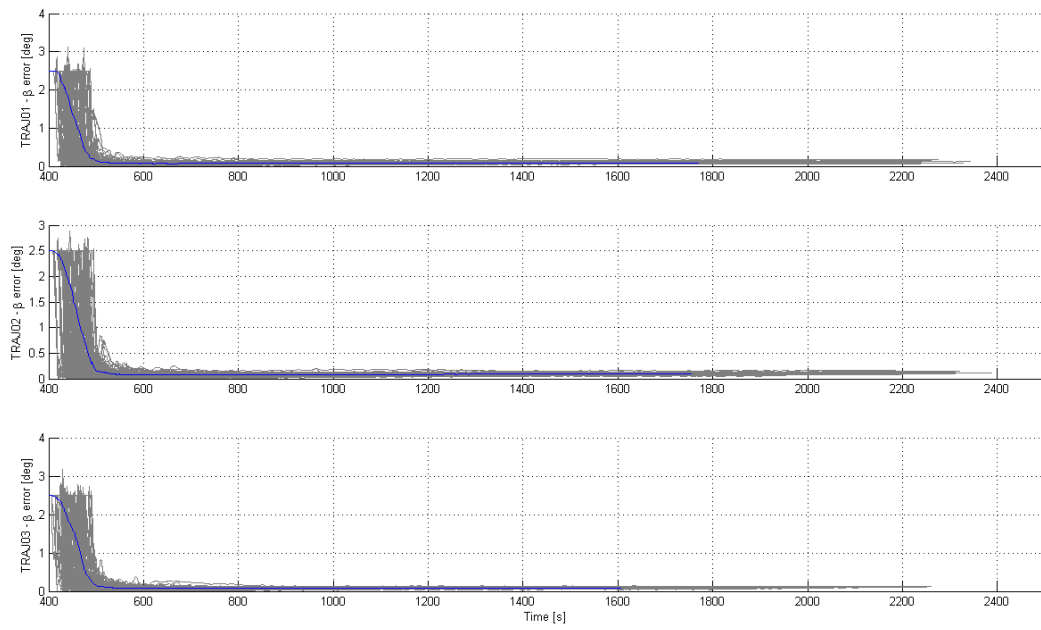


Figure 13:  $\beta$  misalignment angle estimation error in each test.

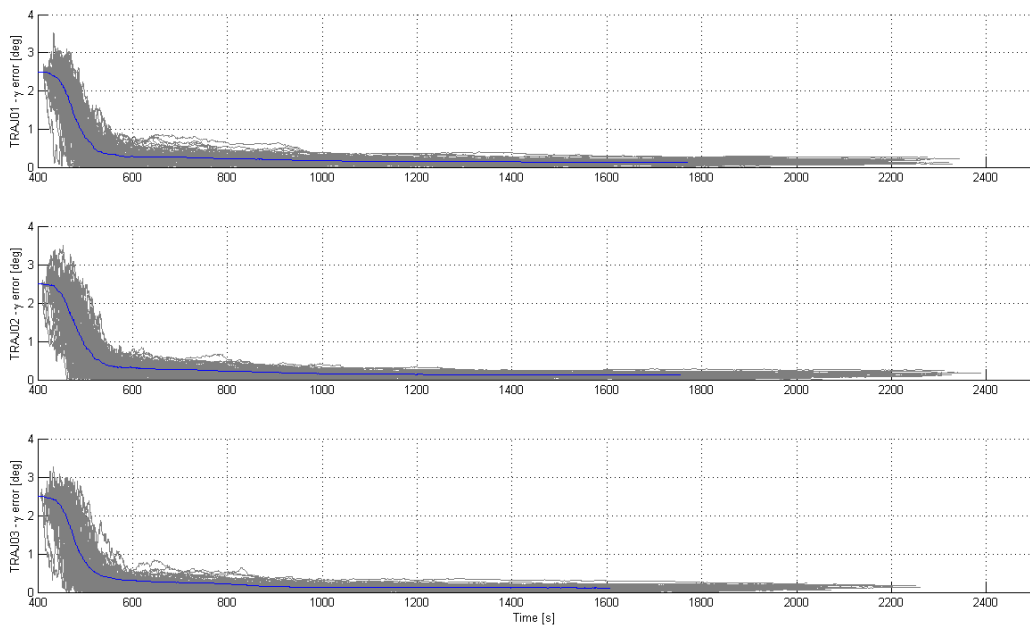


Figure 14:  $\gamma$  misalignment angle estimation error in each test.

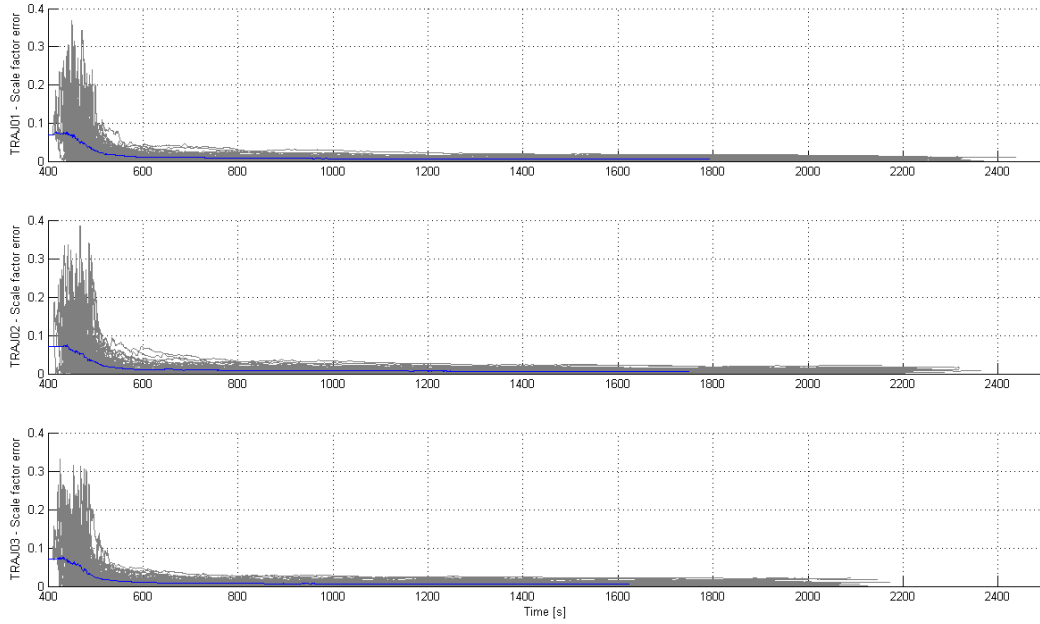


Figure 15: Scale factor estimation error in each test.

Again, with TRAJ03 we achieves the best estimation of both DVL misalignment angles and scale factor.

Trajectory	Mean [deg]	Standard Deviation [deg]
TRAJ01	0.38	0.14
TRAJ02	0.37	0.14
TRAJ03	0.35	0.15

Table 5: Norm of misalignment angles estimation error: mean and standard deviation (2<sup>nd</sup> test set).

Trajectory	Mean	Standard Deviation
TRAJ01	0.0064	0.0046
TRAJ02	0.0059	0.0045
TRAJ03	0.0058	0.0042

Table 6: Scale factor estimation error: mean and standard deviation (2<sup>nd</sup> test set).

## 4. Experimental results and surface position estimation

### 4.1. Sea calibration test

The results shown below refer to the test conducted out of harbour with a manned underwater vehicle.

Sensor	Output Rate	Variable	Accuracy
INS	100 Hz	Heading	0.2 ° sec(lat)
		Roll/Pitch	0.1 °
DVL	> 1 Hz	Velocity	0.4% ± 2 mm/s
GNSS receiver	1 Hz	Position	10 m

Table 7: Submarine sensors specifications.

An operator that conducts the vehicle (with the aid of the GPS and a display) performs the calibration trajectory. The curves are performed keeping the steering angle constant, while the straight lines are carried out maintaining a constant direction.

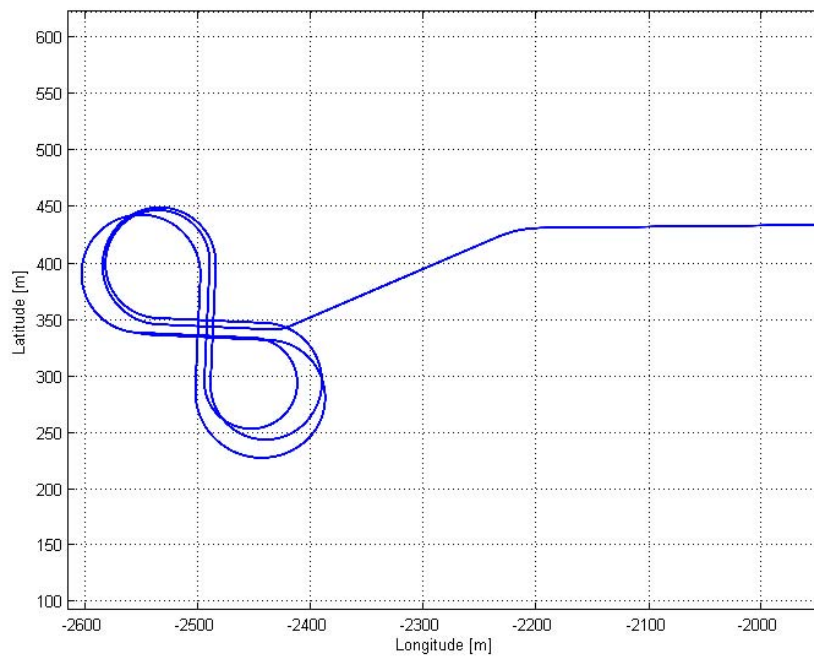


Figure 16: 2D position plot of calibration surface trajectory.

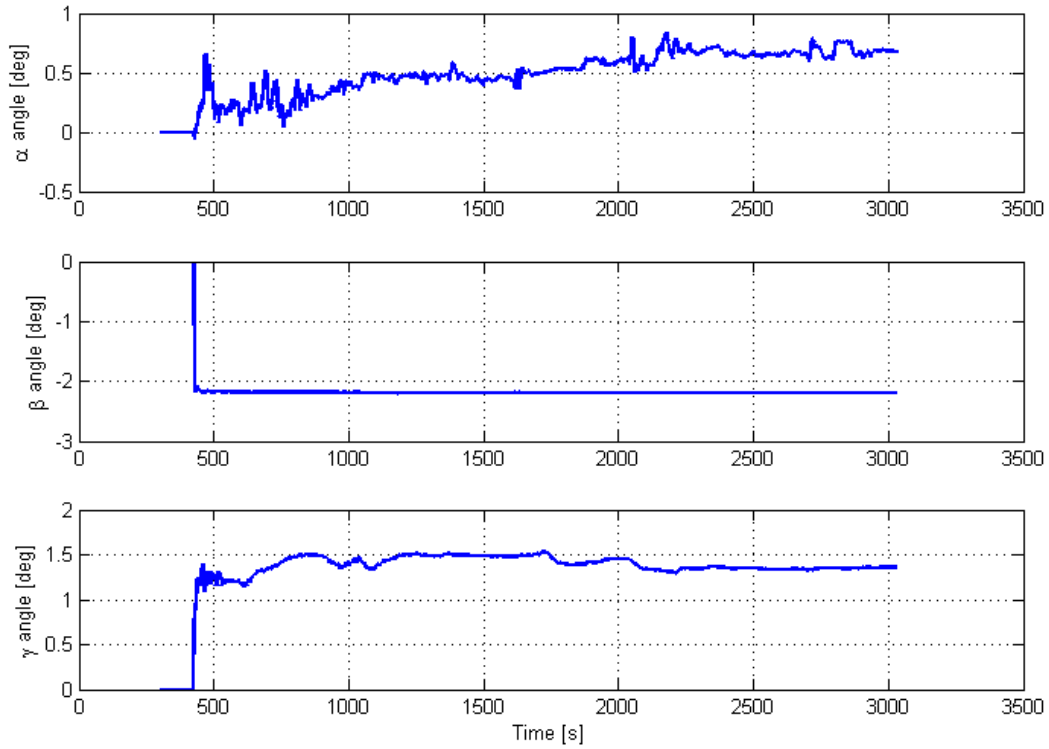


Figure 17: DVL misalignment angles convergence. The  $\alpha$  angle is the slowest estimated angle because of poor observability along body lateral direction.

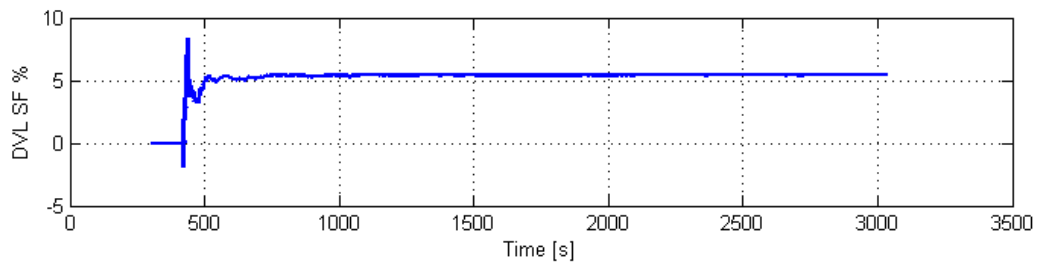


Figure 18: DVL scale factor convergence.

DVL $\alpha$ misalignment	0.69°
DVL $\beta$ misalignment	-2.19°
DVL $\gamma$ misalignment	1.36°
DVL scale factor	5.4%

Table 8: Estimated DVL misalignment angles and SF at the end of calibration.

#### 4.2. Surface position estimation in a sea test

This section shows the acquired INS data and the simulated trajectory with no DVL calibration parameters. If the calibration parameters are correct, then the INS has to



estimate a better position. The sea test has two sub-test intervals (S1, S2) in which the GPS is disconnected from INS but is always acquired. We evaluate the position error when the GPS is connected again, and we compare the INS-calculated position with the mean of the GPS fix in the successive 10 seconds.

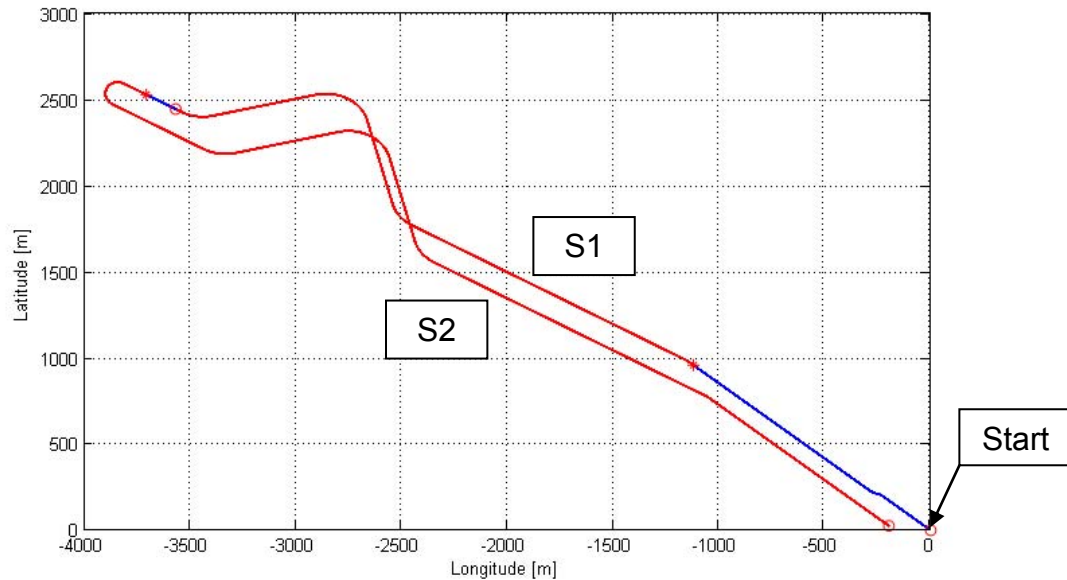


Figure 19: 2D GPS position starting at (0,0). We indicate with blue lines the positions where GPS is connected and with red lines the positions where the GPS is disconnected.

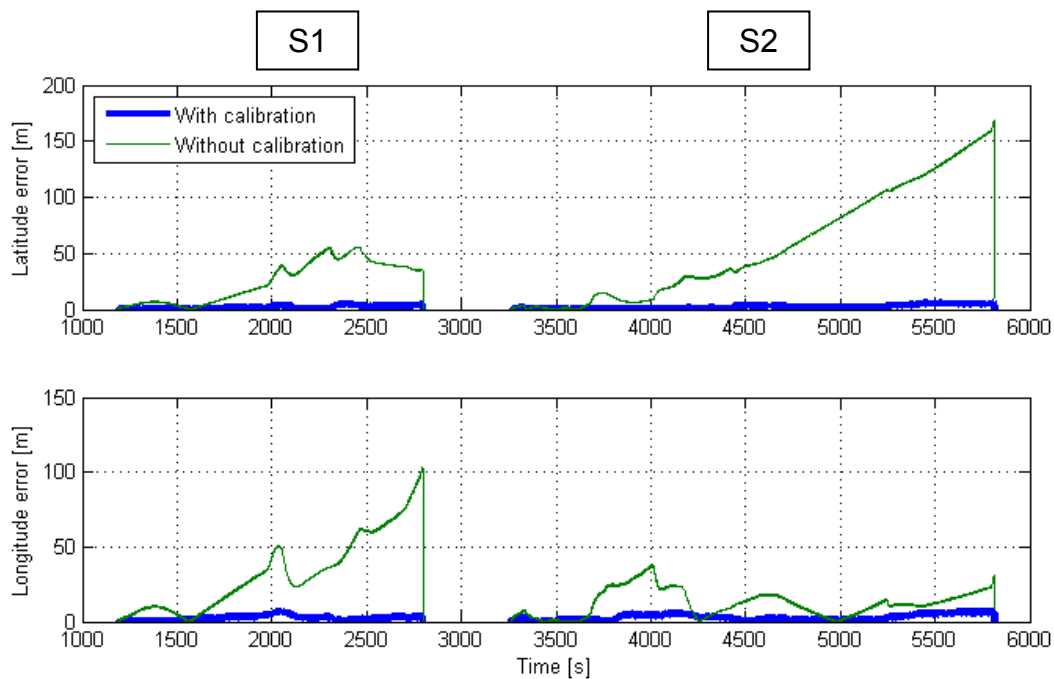


Figure 20: Latitude and longitude error plots in meters with respect to GPS data.

	S1		S2	
Max Horizontal Position Error [m]	N	E	N	E
INS without DVL calibration	56	102	167	38
INS with DVL calibration	5	7	6	7

Table 9: Comparison of horizontal position error in meters.

Horizontal Position Error to DT	S1	S2
INS without DVL calibration	3.8%	3.5%
INS with DVL calibration	0.3%	0.2%

Table 10: Comparison of position error with respect to distance travelled (DT).

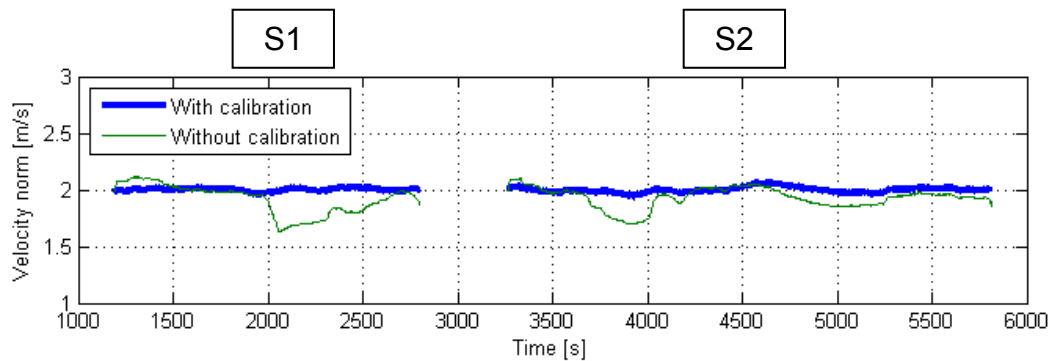


Figure 21: Velocity norm comparison.

Norm Velocity Error (Std Dev) [m/s]	S1	S2
INS without DVL calibration	0.132	0.089
INS with DVL calibration	0.013	0.023

Table 11: Comparison of velocity error. We obtained these results with and without DVL calibration.

## 5. Conclusion

Even if there are many studies that use observability theory to calibration problem, we use a simulative-experimental approach.

We show that our calibration algorithm let us achieve definitely better performance in the sea test respect to a non-calibrated navigation.

More precisely, after calibration we obtain a position error less than 0.3% of the distance travelled.

Moreover we reach this result without the aid of other sensors usually used in submarine navigation, as USBL (Ultra-Short Baseline) or LBL (Long Baseline). The integration with these sensors will be the subject of future research.

## **References**

- [1] IEEE Aerospace and Electronics Systems Society, "IEEE Standard for Inertial Systems Terminology", IEEE, New York, 2009
- [2] M. S. Grewal and A. P. Andrews, "Kalman Filtering: Theory and Practice using MATLAB", 3<sup>rd</sup> Edition, John Wiley & Sons, Inc., 2008
- [3] P. D. Groves, "Principles of GNSS, Inertial and Multisensor Integrated Navigation Systems", 2<sup>nd</sup> Edition, Artech House, 2013
- [4] R. M. Rogers, "Applied mathematics in integrated navigation systems", AIAA Education Series, 2003
- [5] M. F. Abdel-Hafez and J. L. Speyer, "Observability of an integrated GPS/INS during manoeuvres" in IEEE Trans. Aerosp. Electron. Syst., vol. 40, no. 2, pp. 526–535, 2004.
- [6] Y. F. Jiang and Y. P. Lin, "Error estimation of INS ground alignment through observability analysis" in IEEE Trans. Aerosp. Electron. Syst., vol. 28, no. 1, 1992.